Studies in Conservation

Received 11 Jan 2017, Accepted 05 Jul 2017, Published online: 01 Aug 2017
http://dx.doi.org/10.1080/00393630.2017.1353282

Original research or treatment paper

FTIR measurement of cellulose microfibril angle in historic Scots pine wood and its use to detect fungal decay

Kate Hudson-McAulay[a*], David Auty[b], Michael C Jarvis[a†]

[a]*School of Chemistry, Glasgow University, Glasgow G12 8QQ, Scotland, UK.*

[b]*School of Forestry, Northern Arizona University, Flagstaff, Arizona 86011, USA.*

[*]Present address: *North Somerset Council, Town Hall, Walliscote Grove Road, Weston-super-Mare, BS23 1UJ.*

[†]Corresponding author. Email mikej@chem.gla.ac.uk

Abstract

Microfibril angle (MFA) - the orientation of cellulose fibres in the S2 layer of the secondary cell wall - is a key determinant of the stiffness and strength of timber. The microfibril angle depends on the way in which the timber was grown and its position within the tree. Microfibril angle can be measured by X-ray diffraction and other methods, but the methods in current use are slow or require advanced instrumentation. The aim of this study was to explore the use of polarised Fourier transform infrared (FTIR) microscopy as a relatively fast and inexpensive method for measuring MFA in historic Scots pine (*Pinus sylvestris* L.). The FTIR measurements were calibrated against X-ray measurements of MFA in modern Scots pine. We observed a wide range in MFA values and a radial pattern of MFA similar to modern Scots pine in un-decayed Scots pine heartwood from 16th and 17th Century beams in Scottish secular buildings. The density of the heartwood was also similar to modern plantation-grown Scots pine despite the much slower growth rate recorded in the ring widths of the historic timber. The sapwood, which had been attacked by both insect pests and fungi, showed an erratic reduction in density and a large increase in MFA compared to the modern material. The increased sapwood MFA was attributed to selective destruction of the S2 layer of the wood cell walls by fungal decay. Using MFA measurements in conjunction with density offers the possibility to estimate the mechanical properties of sound historic pine timber, to detect fungal decay more sensitively than density alone and to distinguish between pest and fungal attack in a way that relates directly to the remaining mechanical performance of the timber.

Keywords: Wood; infrared spectroscopy; brown rot; cell-wall

The research described here was funded through a PhD studentship awarded to the University of Glasgow by Historic Scotland.

No financial benefit to the authors has arisen from the direct application of this research.

Introduction

It can be difficult to reconcile the need to ensure the structural integrity of historic buildings that are open to the public with the authenticity of these monuments as parts of our heritage. Typically, although strong enough to have survived until the present day, historic buildings were not designed according to modern engineering criteria. Timber buildings, and timber structures within buildings, present particular difficulties because each structural member withstands a wider range of mechanical stresses than brick or stone, may flex to a degree that makes computational mechanics challenging (Hume, 2007), and may periodically need repairs that combine the restoration of load-bearing capacity with respect for the original structure (Hume, 2007; Norris, 2007).

Timber is quite well understood as a modern building material, and information on the mechanical performance and durability of major timber species is generally accessible (Van Acker et al., 2003; Wegst & Ashby, 2004). It has usually been assumed that these properties do not change with time unless the timber is attacked by insect pests or fungi. The two most important factors connecting the mechanical properties of timber with its molecular and anatomical structure are wood density and the orientation of the cellulose fibres in the secondary cell wall, commonly called the microfibril angle or MFA (Lachenbruch et al., 2010; Lichtenegger et al., 1999).

The stiffness and strength of wood are approximately proportional to its density, which depends on the mean thickness of its cell walls (Kostiainen et al., 2009). Each wood cell wall has a layered structure. The outermost layer is known as the primary cell wall, and contains less cellulose and more lignin than the other layers (Burgert et al., 2006). On the inside of the primary wall are three secondary wall layers denoted S1, S2 and S3. In the thin S1 layer the cellulose microfibrils are orientated at a large angle to the grain, around 60°–80° (Donaldson, 2008).The S2 layer, typically between 1 and 10 μm thick, accounts for about 80% of the cell-wall thickness, mass and mechanical strength. Its microfibrils are laid down in a helical pattern at an angle that in softwoods is usually 10°-30° to the grain (Barnett & Bonham, 2004; Donaldson, 2008), which gives the wood greater mechanical strength and stiffness along the grain (Hein & Brancheriau, 2011). The innermost, S3 layer of the cell is thin, with cellulose microfibrils at an angle of 60°–90° to the grain (Barnett & Bonham, 2004).

The microfibril angle (MFA) of a wood cell is usually defined as the angle between the cellulose microfibrils in the S2 layer and the grain (Barnett & Bonham, 2004; Donaldson, 2008). The S2 layer is the prime determinant of the longitudinal strength and stiffness of the wood because it is much thicker, and has lower MFA, than the other layers (Barnett & Bonham, 2004; Donaldson, 2008; Khalili et al., 2001). MFA can be measured by a variety of destructive optical and X-ray methods (Auty et al., 2013; Barnett & Bonham, 2004; Evans & Ilic, 2001; Long et al., 2000). The most detailed measurements are obtained by X-ray diffractometery, for example by using the Silviscan-3 instrument (Innventia AB, Stockholm) which can also measure wood density at sub-ring spatial resolution (Evans & Ilic, 2001; Long et al., 2000).Reported values of MFA are dependent on the measurement method, and what is measured differs in some cases from the accepted definition. While some microscopy-based methods do record the angle in the S2 layer (Khalili et al., 2001), X-ray methods record the orientation distribution over the whole thickness of the cell wall, from which the calculation of a single figure is quite complex (Evans & Ilic, 2001). Birefringence or spectroscopic methods like polarized Fourier transform infrared (FTIR) spectroscopy derive a single, integrated figure from the whole orientation distribution in all the cell-wall layers (Leonardon et al., 2010). The domination of the cell-wall thickness by the S2 layer means that differences in MFA values obtained using different methods are normally small.

In Scots pine (*Pinus sylvestris* L.) and other softwood species, there is characteristic variation in wood properties from the centre of the tree to the outside, corresponding to increasing age of the tree at the time when the wood was laid down. The width of the annual rings and the MFA decrease and the density increases with distance from the centre, so that the mechanical properties of sound wood increase towards the outside of the tree (Auty et al., 2014; Auty et al., 2013). The sapwood at the outside, however, is generally more susceptible to biological decay (Meyer & Brischke, 2015).

Density is reduced when wood is attacked by insect pests (Curling et al., 2002; Sousa et al., 2014; Unger et al., 2001). Amongst wood-rotting fungi, the most common brown rots preferentially attack the S2 layer of the wood cell wall, which has lower lignin content and MFA than the other layers (Liese, 1970; Pandey & Pitman, 2004). Loss of cellulose from the S2 layer would therefore be expected to increase the mean microfibril angle of the affected wood, when measured by any method that derives the MFA from the whole orientation distribution of all layers of the cell wall. This principle could potentially be used to detect fungal

decay in a way directly connected to the resulting loss of mechanical integrity. Wood density can either be calculated using measurements of volume and mass, or measured by X-ray densitometry at the spatial resolution needed to record the density variation across annual rings (Evans & Ilic, 2001).

Due to the high cost of measuring MFA by X-ray diffraction (e.g. using Silviscan-3), simpler methods for measuring MFA are preferred when lower spatial resolution is required. Polarised FTIR microscopy, which can be performed on thin sections of wood (Faix et al., 1992; Krauss & Kudela, 2011) can detect variation in MFA at low cost, but has not previously been calibrated for quantitative use.

The aims of this study were to calibrate the FTIR measurement of MFA in 16th and 17th Century Scots pine and to investigate the effects of pest and fungal decay. A simple method of measuring MFA in the very small samples that are normally available from historic structures would facilitate the structural assessment of these structures and the choice of modern timber matching the properties of components in need of replacement.

Historic and Modern Wood Samples

Sixteenth and Seventeenth Century samples of Scots pine were obtained from the beam ends of painted ceilings in three Scottish buildings. Details of the history of these three buildings and of the dendrochronological examination of the same beam ends are given by Crone et al. (2017). The Abbey Strand Sanctuary is a three storey building in Edinburgh dating to the late 16th / early 17th century (Historic Scotland, 2012). The Bay Horse Inn in Dysart, Fife is a compact two story domestic building which is dated to 1583. Its painted ceilings have a dendrochronological date in the 16th century (Crone et al. 2017). Carnock house was originally a simple rectangular building with two stair towers, built in 1548 by Robert Drummond (Canmore, 2013). Its painted ceiling has been dendrochronologically dated to 1588-1589 (Crone et al. 2017). A total of six Scots pine beams from these buildings were examined. At the time when these buildings were constructed the pinewoods of the Scottish Highlands were exploited predominantly for local use and Scots pine for buildings constructed in lowland Scotland was mostly imported from Scandinavia; a detailed description of trade routes is given by Crone & Mills (2012).

Many, but not all of the historic samples had visible signs of insect pest damage, restricted to the sapwood that was located mainly at the corners of the beams.

Modern Scots pine samples for the calibration of the MFA measurements were obtained from four commercial plantations in Scotland and processed as described by Auty et al (2013). Modern samples for comparison of density were obtained commercially, originating from similar plantations in Northeast Scotland.

Experimental Procedures

Ring width

Annual ring width measurements had already been measured on the calibration samples, based on X-ray densitometry (Auty et al., 2013). Ring widths were measured optically on the historic samples.

Density

Volumetric wood density measurements for the historic pine were taken on 5 mm cubic samples, which were cut in radial series from the edge of each beam nearest the pith to the sapwood edge. Longitudinal-radial sections of nominal thickness 19 µm were cut from these cubes, and from the 2-mm-thick strips on the Silviscan-3 calibration samples (Auty et al., 2013).

The density of the historic samples was measured after drying for 4 h at 110°C and cooling in a dry, sealed chamber. The 5 mm cubes were weighed (nearest 0.1 mg) and measured in each dimension with digital callipers (nearest 0.01 mm).

Polarised FTIR microscopy of thin sections

Before cutting sections the cubes were soaked for 12 h in water to soften the wood (Faix et al., 1992). Axial-tangential sections 19 µm thick were then cut from the blocks using a Leica RM2255 microtome (Leica Biosystems, 69226 Nussloch, Germany) with a steel blade (Fackler & Schwanninger, 2012). FTIR spectra were recorded from 100 µm square fields of the thin sections on a Nicolet Nexxus spectrometer with a Nicolet Continuum microscope attachment (Fisher Scientific UK Ltd, Loughborough, UK) fitted with a ZnSe infrared polariser, as described by Leonardon et al. (2010). The spectra were exported as .csv files into Microsoft Excel and baseline-corrected using a segmented baseline with linear segments joining the minima at 918, 1136, 1538, 1810, 2635, 3003 and 3764 cm^{-1} as described by Altaner et al. (2014).

The FTIR spectrum of wood contains a number of peaks whose intensity is affected by the direction of polarisation of the incident radiation. Since the spectra were recorded in absorbance mode, peak areas were determined by integration. The well-defined 1162 cm^{-1} peak (Figure 1), assignable to stretching of the linkage between successive glucose molecules in the cellulose chain, has a high dichroic ratio (the intensity with parallel polarisation / the intensity with transverse polarisation) and its dichroism has been used qualitatively to estimate the orientation of cellulose (Chang et al., 2014; Schmidt et al., 2006; Stevanic & Salme, 2009). Here the dichroic ratio of the 1162 cm^{-1} peak was used as a measure of MFA.

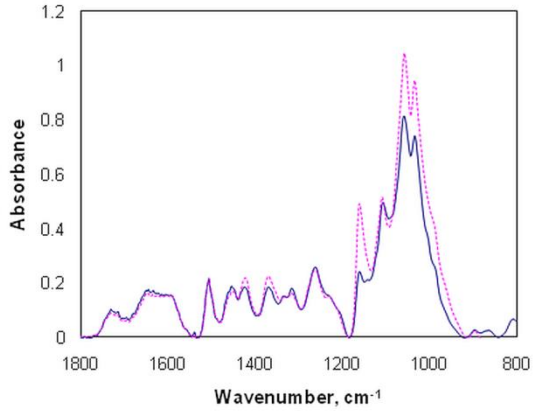

Figure 1: Polarised transmission infrared (FTIR) spectra of Scots pine wood. Red: polarisation parallel to the grain. Blue: transverse polarisation. The ratio of the absorbances of the 1162 cm^{-1} peak in the parallel and transversely polarised spectra is the dichroic ratio for this peak, which is assigned to stretching of the linkages between glucose units in the cellulose chain.

For quantitative work it is necessary to ensure that FTIR spectra are not saturated due to excessive sample thickness. A real sample thickness of 19 µm would certainly lead to saturated spectra but in longitudinal-radial sections, since the sections are less than one cell thick the actual thickness is that of the cell wall. This gave satisfactory, non-saturated absorbances of <1 in the fingerprint region from most of the sections but some spectra from high-density latewood, which has thicker cell walls, were excluded from the calibration due to saturation. Before averaging, the spectra were normalised to equalise the intensity of the 1508 cm^{-1} lignin peak, which had equal absorbance in the parallel and transversely polarised spectra, to avoid increased weighting from sections with higher overall absorbance.

Polarised FTIR spectra were collected from five replicate sections from each of the calibration samples, at 0.5 mm intervals along four separate radial paths. The total number of spectra in the calibration set was approximately 4000. The dichroic ratio of the 1162 cm^{-1} peak was averaged between 1153 cm^{-1} and 1169 cm^{-1} after baseline correction. The dichroic ratios were then sorted according to ring number and averaged for each annual ring for comparison with the MFA data measured by X-ray diffractometry on the same sample strips (Auty et al., 2013)

From each of the six historic beam ends, three 5 mm cubes were prepared from the inner heartwood nearest the pith, the outer heartwood and the sapwood. Microtome sections were cut from the radial-longitudinal face of each cube and FTIR spectra with longitudinal and transverse polarisation were collected at 0.5 mm intervals along four replicate radial paths in each section. Thus approximately 40 pairs of polarised spectra were obtained for each cube and the total number of spectra was comparable with the calibration set.

Results

Ring width.

The historic samples all had much narrower rings than are found in modern plantation-grown Scots pine (Figure 2) indicating slower radial growth, as would be expected in a semi-natural forest environment (Chang et al., 2014), and it would be quite difficult to source wood with a similarly slow growth rate today. It might therefore be expected that the density of the historic material would be higher and its microfibril angle lower, leading to higher stiffness (Barnett & Bonham, 2004). Density and microfibril angle were measured to test this hypothesis.

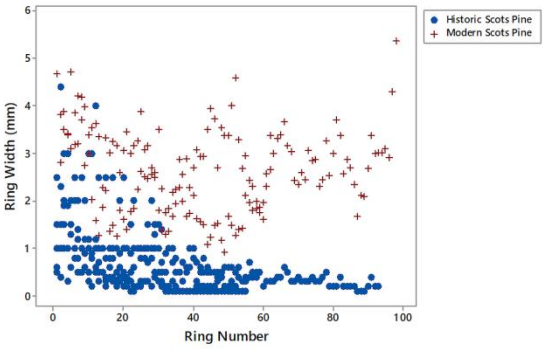

Figure 2: Ring width plotted against ring number from the centre of the tree, for modern and historic Scots pine.

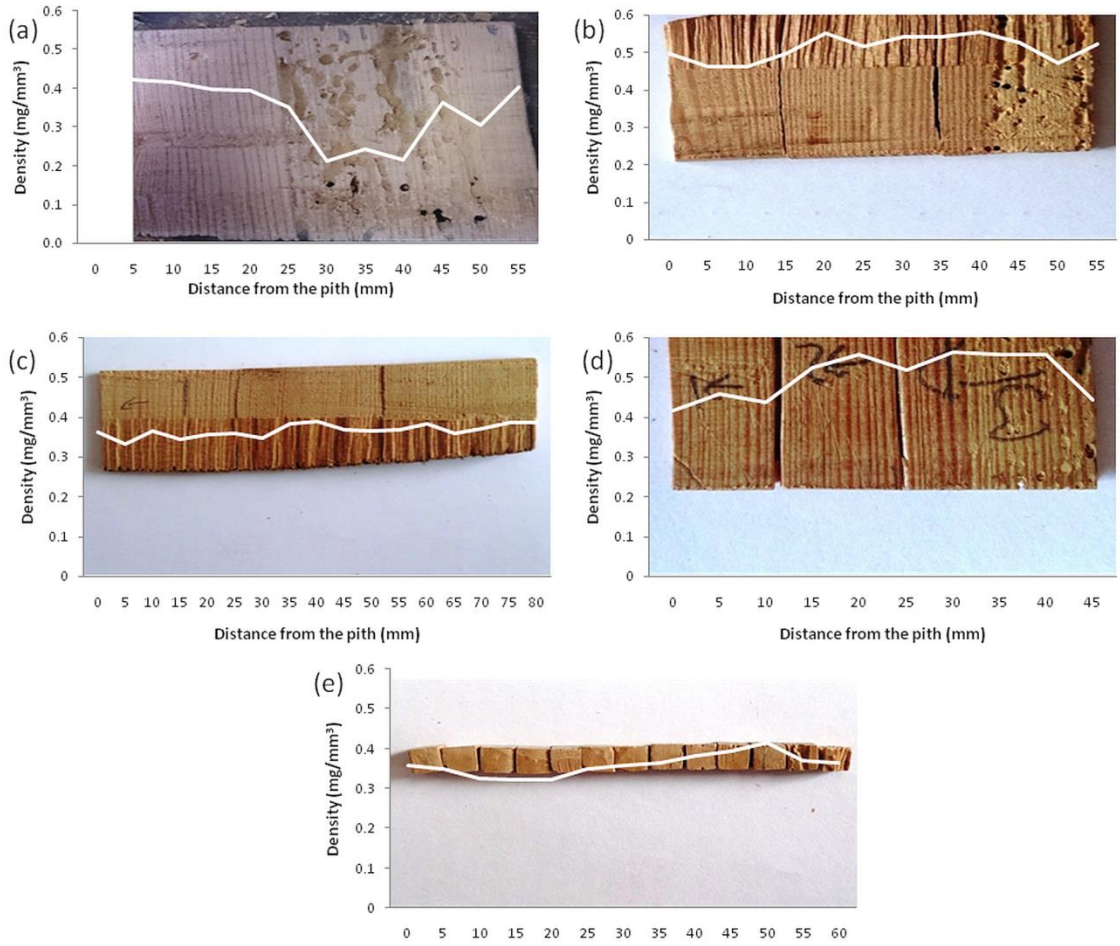

Figure 3: Radial variation in density of five historic Scots pine beams (A-E), superimposed on cross-sectional images. Sapwood showing varying degrees of pest damage on right.

Density

Scots pine wood density has a distinctive pattern of radial variation, starting with relatively low values close to the pith, and rapidly increasing before reaching stable values in the mature wood (Auty et al., 2013). Most of the historic samples showed density profiles corresponding to this pattern but where the sapwood contained pest holes there was a reduction in density at the sapwood edge (Figure 3).

There was considerable tree-to-tree variation in the density of the historic samples. The mean density of the historic samples was lower than that of the modern samples used for comparison (*t*-test, $P<0.001$). However, when heartwood samples only were compared, no significant differences were found, indicating that differences in density between the historic and modern samples were due to the visible loss of mass in the decayed sapwood of the historic samples.

Microfibril angle: calibration of polarised FTIR method against Silviscan-3 X-ray diffraction measurements on modern Scots pine

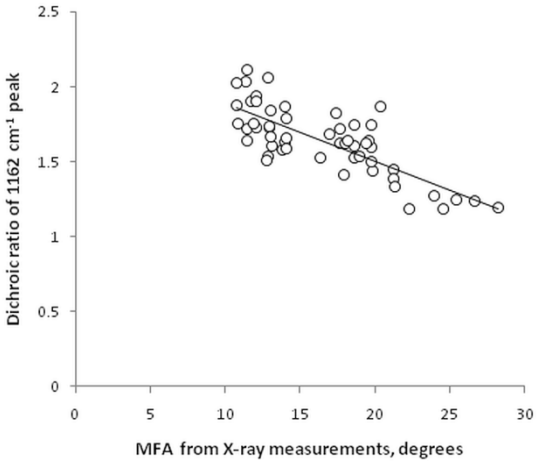

Figure 4: Calibration plot of the dichroic ratio (peak area longitudinal / peak area transverse) for the 1162 cm^{-1} peak in the polarised FTIR spectrum against the microfibril angle (MFA) in degrees, obtained by X-ray diffraction.

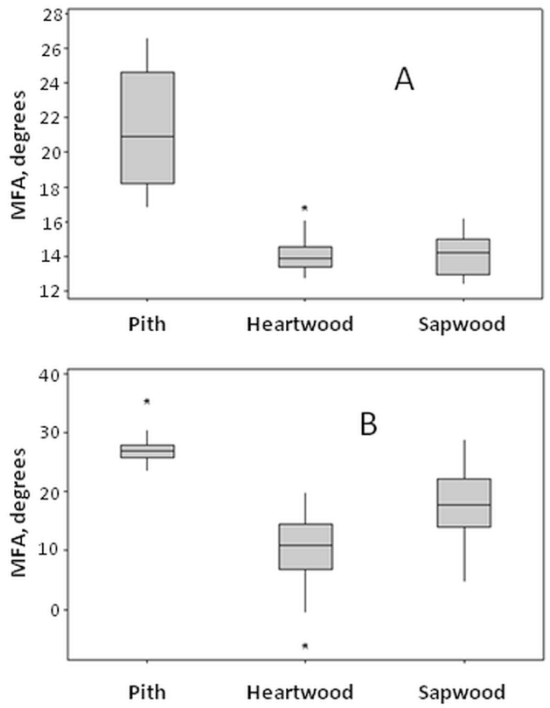

Figure 5: Box plots of cellulose orientation at different radial positions for Scots pine wood. A; derived from the X-ray diffraction measurements on the modern calibration set. B; averaged for five historic samples, measured by FTIR with calibration from X-ray diffraction.

The calibration of the polarised FTIR procedure covers MFA values ranging from 10° to 30° as measured by X-ray diffraction (Figure 4) and was fitted with a simple linear relationship with an R^2 value of 0.60 based on annual ring averages ($P < 0.001$). Although in theory a degree of non-linearity might be expected (Cowdrey & Preston, 1966), this would probably become more evident if the calibration were extended to include lower MFA values.

MFA in historic Scots pine

Figure 5B shows boxplots of mean cellulose orientation in the six historic Scots pine samples, obtained from the polarised FTIR spectra calibrated against the modern samples analysed by X-ray diffractometry. One heartwood sample had a mean dichroic ratio beyond the calibration range and its inclusion required the assumption that the calibration range can be extrapolated linearly when MFA < 10°. One-way analysis of variance (ANOVA) showed a significant effect of radial position (inner heartwood at the end closest to, and in some samples including, the pith; outer heartwood and sapwood) on cellulose orientation for the whole data set ($P< 0.001$). Multiple comparison tests for least significant differences using both Tukey and Fisher criteria showed that each radial position was significantly different from the others for the whole historic sample set. The less axial cellulose orientation (resembling an increase in MFA) in the sapwood was statistically significant ($P< 0.05$) in four of the six individual sapwood samples tested.

Estimation of wood stiffness from microfibril angle and density

In theory, approximate values of wood stiffness can be predicted from the density and MFA of clear (knot-free and un-decayed) wood. Previously, a simple equation of the form $MOE = k_1 (D/MFA) + k_2$, where MOE is the modulus of elasticity and k_1 and k_2 are constants, has been used (Hein et al., 2013) to estimate the longitudinal MOE from MFA and density (D). A more complex approach is used in the Silviscan-3 software to calculate MOE directly from the X-ray density and diffraction patterns (Evans & Ilic, 2001). Plotting D/MFA against MOE for the calibration set gave a linear relationship ($R^2 = 0.92$) with $k_1 = 0.30$ and $k_2 = 2.22$, allowing estimates of the average stiffness of the historic samples from the gravimetric density and the MFA measured by FTIR. These estimates ranged from 6 Gigapascals (GPa) close to the pith, up to 13 GPa in the heartwood. The heartwood sample with MFA below the lower limit of the calibration range was excluded here because low MFA, in the denominator, has an excessive influence on the D/MFA ratio. Predicting the MOE of the sapwood in this way would not meaningful due to the selective loss through decay of the S2 layer of the cell wall.

Discussion

The ring width measurements showed that the historic pine samples were much slower-grown than typical modern timber. Nevertheless, the density and MFA values recorded in the heartwood of the historic pine beams were not exceptionally different from those in the modern samples and could be used together to predict elastic moduli within the range obtainable today in commercially available Scots pine (Auty & Achim, 2008), on the assumption that there had been no reduction in stiffness in the historic pine samples over time. This assumption is tested in the accompanying manuscript (Hudson-Macaulay and Jarvis, submitted).

In Scots pine, density generally increases with distance from the centre of the tree, levelling off around annual ring 20-30 (e.g. Auty et al. (2014)). Temporary decreases in density can be associated with periods of faster radial growth that produce wider annual rings (Auty et al., 2014), for example after thinning. In this study, the decrease in sapwood density in the historic Scots pine samples is unlikely to be attributable to such temporary causes because it was observed in a range of samples of different ages. The most likely cause of the decreased density in the sapwood, therefore, was the visible decay with which it was associated. Pest holes obviously decrease the density of wood but fungi are also likely to cause a decrease in density by degrading and metabolising the carbohydrate polymers (Enoki et al., 1988; Hastrup et al., 2012). Both forms of decay may therefore have contributed to the loss of density, but their relative contributions cannot be determined from the density measurements alone.

Microfibril angle in Scots pine is typically high at the centre of the tree, falls with distance from the centre until about annual ring 20, and then remains approximately constant. Illustrating this typical pattern, Figure 5A is derived from the calibration X-ray data set (Auty et al., 2013) reorganised to match the sampling of the historic material. In contrast the historic samples showed a large increase in axial cellulose orientation in the sapwood (Figure 5B) which was significant in four of the six historic samples tested. A local increase in MFA can be associated with wide annual rings (Auty et al., 2013) but the observed increase in axial cellulose orientation in the sapwood, atypical for Scots pine, is unlikely to be a local effect of rapid growth since there was no evidence of increased ring width in the sapwood (Figure 2).

There is no evident reason for the orientations of individual microfibrils to change over time after the tree is felled, or as a result of pest damage or fungal decay. However selective destruction of the S2 layer of the wood cell walls by fungi would be expected to increase the mean angle between the microfibrils and the grain direction, because the remaining, more resistant cell-wall layers all have their cellulose microfibrils orientated at a greater angle to the grain. The polarised FTIR data reported here are consistent with that explanation.

Strictly, the resulting microfibril orientation does not correspond to the microfibril angle when that is defined as the angle of the microfibrils in the S2 layer of the cell wall. However all layers of the cell wall contribute to the infrared dichroic ratio measured here, to the diffraction patterns from which the X-ray estimate of MFA is derived and to the mechanical properties of the wood (Wagner et al., 2014). No such effect on MFA would be expected from pest damage because pest holes are created by the destruction of all layers of the wood cell wall.

The selective detection of fungal decay in this way has the advantage that the cellulose orientation measured is directly connected with the mechanical performance of the wood. The selective loss of the well-oriented cellulose in the S2 layer implies a greater reduction in stiffness and strength than would be expected from lower density alone, and might also imply altered anisotropic shrinkage (Harris & Meylan, 1965) in the changing humidity of historic outdoor structures. Even combining the negative effects of reduced density and less axially-oriented cellulose, the loss of stiffness would still be underestimated, as fungal decay also depolymerises the cellulose and other polymers that remain (Wagner et al., 2014).

Conclusions

When correctly calibrated, polarised FTIR microscopy can be used to measure the orientation of cellulose fibres in small samples of historic wood. These measurements, in conjunction with simple measurements of density or with densitometric measurements made for the purpose of paleoclimate reconstruction (Wilson et al. 2012), can be used to infer details of how the growth environment of the wood might have influenced its mechanical properties. Polarised FTIR measurement of cellulose orientation might also be used to provide a sensitive method of detecting when wood has been weakened by fungal decay.

Acknowledgements

The authors thank Historic Scotland for funding this work and for providing access to the historic wood material. Dr Craig Kennedy (then at Historic Scotland) and Dr Anne Crone (AOC Archaeology) are thanked for their inputs in the planning of the experiments on historic pine. The X-ray diffraction measurements on modern wood were funded by the Scottish Forestry Trust, the Forestry Commission and EC COST Actions EC50 and FP0802.

References

Altaner, C.M., Thomas, L.H., Fernandes, A.N., Jarvis, M.C. 2014. How cellulose stretches: synergism between covalent and hydrogen bonding. *Biomacromolecules*, **15**(3), 791-798.

Auty, D., Achim, A. 2008. The relationship between standing tree acoustic assessment and timber quality in Scots pine and the practical implications for assessing timber quality from naturally regenerated stands. *Forestry*, **81**(4), 475-487.

Auty, D., Achim, A., Macdonald, E., Cameron, A.D., Gardiner, B.A. 2014. Models for predicting wood density variation in Scots pine. *Forestry*, **87**(3), 449-458.

Auty, D., Gardiner, B.A., Achim, A., Moore, J.R., Cameron, A.D. 2013. Models for predicting microfibril angle variation in Scots pine. *Annals of Forest Science*, **70**(2), 209-218.

Barnett, J.R., Bonham, V.A. 2004. Cellulose microfibril angle in the cell wall of wood fibres. *Biological Reviews*, **79**(2), 461-472.

Burgert, I., Keckes, J., Fratzl, P. 2006. Mechanics of the wood cell wall. In Stokke, D. D.

Groom, L. H. (Eds) *Characterization of the Cellulosic Cell Wall.* 30-37.

Canmore. 2013. Dysart, Panhall, 1 Pan Ha', Bay House [Online]. [Accessed 04/04/13] Available from: http://canmore.org.uk/site/53989/dysart-panhall-1-pan-ha-bay-house

Chang, S.-S., Salmen, L., Olsson, A.-M., Clair, B. 2014. Deposition and organisation of cell wall polymers during maturation of poplar tension wood by FTIR microspectroscopy. *Planta*, **239**(1), 243-254.

Cowdrey, D.R., Preston, R.D. 1966. Elasticity and microfibrillar angle in wood of Sitka spruce. *Proceedings of the Royal Society Series B-Biological Sciences*, **166**(1004), 245-272.

Crone, A., Bath, M., Pearce, M. 2017. *The Dendrochronology and Art History of a Sample of 16th and 17th Century Painted Ceilings*. Research Report, Historic Environment Scotland, Edinburgh.

Crone, A., Mills, C.M. 2012 Timber in Scottish buildings, 1450–1800; a dendrochronological perspective. *Proceedings of the Society of Antiquaries of Scotland* 142, 329–69.

Curling, S.F., Clausen, C.A., Winandy, J.R. 2002. Experimental method to quantify progressive stages of decay of wood by basidiomycete fungi. *International Biodeterioration & Biodegradation*, **49**(1), 13-19.

Donaldson, L. 2008. Microfibril angle: measurement, variation and relationships - a review. *IAWA Journal*, **29**(4), 345-386.

Enoki, A., Tanaka, H., Fuse, G. 1988. Degradation of lignin-related compounds, pure cellulose and wood components by white-rot and brown-rot fungi. *Holzforschung*, **42**(2), 85-93.

Evans, R., Ilic, J. 2001. Rapid prediction of wood stiffness from microfibril, angle and density. *Forest Products Journal*, **51**(3), 53-57.

Fackler, K., Schwanninger, M. 2012. How spectroscopy and microspectroscopy of degraded wood contribute to understand fungal wood decay. *Applied Microbiology and Biotechnology*, **96**(3), 587-599.

Faix, O., Bottcher, J.H., Bertelt, E. 1992. Using FTIR spectroscopy and FTIR microscopy for the examination of wood and wood tissue *8th International Conference on Fourier Transform Spectroscopy* 428-430.

Harris, J.M., Meylan, B.A. 1965. Influence of microfibril angle on longitudinal and tangential shrinkage in *Pinus radiata*. *Holzforschung*, **19**(5), 144-154.

Hastrup, A.C.S., Howell, C., Larsen, F.H., Sathitsuksanoh, N., Goodell, B., Jellison, J. 2012. Differences in crystalline cellulose modification due to degradation by brown and white rot fungi. *Fungal Biology*, **116**(10), 1052-1063.

Hein, P.R.G., Brancheriau, L. 2011. Radial variation of microfibril angle and wood density and their relationships in 14 year old *Eucalyptus urophylla* St. Blake wood. *Bioresources*, **6**(3), 3352-3362.

Hein, P.R.G., Silva, J.R.M., Brancheriau, L. 2013. Correlations among microfibril angle, density, modulus of elasticity, modulus of rupture and shrinkage in 6 year old *Eucalyptus urophylla* x *E. grandis*. *Maderas-Ciencia Y Tecnologia*, **15**(2), 171-182.

Historic Scotland, 2012. Holyrood Abbey [Online].[Accessed 06/06/12] Available from: http://www.historic-scotland.gov.uk/propertyresults/propertydetail.htm?PropID=PL_124

Hudson-Macaulay, K., Jarvis, M.C. Chemical and mechanical changes in Scots pine wood over historical time (accompanying manuscript).

Hume, I. 2007. The effects of road traffic vibration on historic buildings. *Structures & Construction in Historic Building Conservation*, 223-225.

Khalili, S., Nilsson, T., Daniel, G. 2001. The use of soft rot fungi for determining the microfibrillar orientation in the S2 layer of pine tracheids. *Holz Als Roh-Und Werkstoff*, **58**(6), 439-447.

Kostiainen, K., Kaakinen, S., Saranpaa, P., Sigurdsson, B.D., Lundqvist, S.-O., Linder, S., Vapaavuori, E. 2009. Stem wood properties of mature Norway spruce after 3 years of continuous exposure to elevated CO_2 and temperature. *Global Change Biology*, **15**(2), 368-379.

Krauss, A., Kudela, J. 2011. Ultrasonic wave propagation and Young's modulus of elasticity along the grain of Scots pine wood (*Pinus sylvestris* L.) varying with distance from the pith. *Wood Research*, **56**(4), 479-488.

Lachenbruch, B., Johnson, G.R., Downes, G.M., Evans, R. 2010. Relationships of density, microfibril angle, and sound velocity with stiffness and strength in mature wood of Douglas-fir. *Canadian Journal of Forest Research-Revue Canadienne De Recherche Forestiere*, **40**(1), 55-64.

Leonardon, M., Altaner, C.M., Vihermaa, L., Jarvis, M.C. 2010. Wood shrinkage: influence of anatomy, cell wall architecture, chemical composition and cambial age. *European Journal of Wood and Wood Products*, **68**(1), 87-94.

Lichtenegger, H., Reiterer, A., Stanzl-Tschegg, S.E., Fratzl, P. 1999. Variation of cellulose microfibril angles in softwoods and hardwoods - A possible strategy of mechanical optimization. *Journal of Structural Biology*, **128**(3), 257-269.

Liese, W. 1970. Ultrastructural aspects of woody tissue disintegration. *Annual Review of Phytopathology*, **8**, 231-258.

Long, J.M., Conn, A.B., Batchelor, W.J., Evans, R. 2000. Comparison of methods to measure fibril angle in wood fibres. *Appita Journal*, **53**(3), 206-209.

Meyer, L., Brischke, C. 2015. Fungal decay at different moisture levels of selected European-grown wood species. *International Biodeterioration & Biodegradation*, **103**, 23-29.

Mills, C., Crone, A. 1998. Tree-ring evidence for the historic timber trade and woodland exploitation in Scotland. *Proceedings of the International Conference: Dendrochronology and Environmental Ttrends, 17-21 June, 1998, Kaunas, Lithuania*, 43-55.

Norris, P. 2007. The Building Regulations and related legislation. In M. Forsyth (Ed.) *Structures & Construction in Historic Building Conservation.* 19-40.

Pandey, K.K., Pitman, A.J. 2004. Examination of the lignin content in a softwood and a hardwood decayed by a brown-rot fungus with the acetyl bromide method and Fourier transform infrared spectroscopy. *Journal of Polymer Science Part A-Polymer Chemistry*, **42**(10), 2340-2346.

Schmidt, M., Gierlinger, N., Schade, U., Rogge, T., Grunze, M. 2006. Polarized infrared microspectroscopy of single spruce fibers: Hydrogen bonding in wood polymers. *Biopolymers*, **83**(5), 546-555.

Sousa, H.S., Branco, J.M., Lourenco, P.B. 2014. Prediction of global bending stiffness of timber beams by local sampling data and visual inspection. *European Journal of Wood and Wood Products*, **72**(4), 453-461.

Stevanic, J.S., Salme, L. 2009. Orientation of the wood polymers in the cell wall of spruce wood fibres. *Holzforschung*, **63**(5), 497-503.

Unger, A., Schniewind, A.P., Unger, W. 2001. Biological deterioration of wood. *Conservation of Wood Artifacts*, 51-141.

Van Acker, J., Stevens, M., Carey, J., Sierra-Alvarez, R., Militz, H., Le Bayon, I., Kleist, G., Peek, R.D. 2003. Biological durability of wood in relation to end-use - Part 1. Towards a European standard for laboratory testing of the biological durability of wood. *Holz Als Roh-Und Werkstoff*, **61**(1), 35-45.

Wagner, L., Bader, T.K., Eberhardsteiner, J., de Borst, K. 2014. Fungal degradation of softwood cell walls: Enhanced insight through micromechanical modeling. *International Biodeterioration & Biodegradation*, **93**, 223-234.

Wegst, U.G.K., Ashby, M.F. 2004. The mechanical efficiency of natural materials. *Philosophical Magazine*, **84**(21), 2167-2181.

Wilson, R., Loader, N. J., Rydval, M., Patton, H., Frith, A., Mills, C. M., Crone, A., Edwards, C., Larsson, L., and Gunnarson, B. E. 2012. Reconstructing Holocene climate from tree rings: The potential for a long chronology from the Scottish Highlands. *Holocene* 22 (1):3-11. doi: 10.1177/0959683611405237.